Original Research

Molecular detection and extraction of pyrene in plasma and tissues of Sprague-Dawley rats

C. Bao, X. Dong, J. Tao, J. Lu, T. Luo, J. Liu*

Department of Pathology, Ankang City Central Hospital, No 85, Jinzhou Road, Ankang, Shanxi, China

Abstract: In this paper, an efficient method for determination of total pyrene concentration in the biological samples including plasma, liver, spleen, lung and kidney of Sprague-Dawley rats were investigated and established using steady-state fluorescence method. Equilibrium dialysis method was applied to determine plasma protein binding rate of pyrene. The results illustrated that the protein binding rate depends on the concentration of pyrene in plasma. Extraction of pyrene in plasma was studied by using biomedical nanopartical which was prepared from synthesized associating polymer poly(ethylene glycol) end-capped by hexadecane. The Critical Micelle Concentration (CMC) of the polymeric micelle in aqueous solution was determined to equal 0.0063 mg/mL using 1-pyrenemethanol as a fluorescent probe. The distribution of free pyrene and pyrene loaded nanopartials in blood were determined. The results showed that over 95% of the free pyrene was distributed into the erythrocyte, and the pyrene-loaded nanoparticles were less distributed in to the erythrocyte than free pyrene, but it was higher than 60%. This study provides an efficient method to detect pyrene in different tissues as well as an extraction method at the molecular level, which might contribute to the development of modern molecular diagnosis and identification in vivo.

Key words: Pyrene, biomedical nanopartical, molecular diagnosis, Sprague-Dawley rats.

Introduction

In the past two decades, the rapid development and application of nanotechnology in the field of medicine have changed the knowledge of more and more people to diagnosis, treatment and control of diseases (1,2). Nano-drug, as one efficient approach of molecular therapy and diagnosis, has significant difference with the conventional preparation in physical and chemical properties, as well as pharmacokinetic and pharmacodynamic aspects (3,4). Nano-drug has many advantages to ultimately improve drug efficiency, such as the slow and controlled drug release, targeted drug delivery, improvement of drug bioavailability and therapeutic index etc (2,4-7). The purpose of nano-drug is to reduce adverse drug reactions, and may improve the success rate of drug research, which has become a hot point in the international medical research (1-10). Nano-drug system was prepared by direct nanotechnology of drugs and drug delivery system to achieve nano-drug carrier system, including polymer nanoparticles, solid lipid nanoparticles, microemulsion/submicroemulsion, nano liposome, nano magnetic ball, polymer micelles, dendrimers, inorganic nano carrier, etc (2-6). Polymer nanoparticles are composed of natural polymers such as chitosan, gelatin, sodium alginate and synthetic polymers such as polylactic acid (PLA), poly L-lactide (PLL), poly lactide glycolide (PLG), polycaprolactone (PCL), etc (2,4,6,7,9-15). These polymers can be treated as raw materials to prepare a kind of colloid drug carrier system. The drugs are dissolved, encapsulated and homogeneously dispersed into the matrix of nanoparticles or adsorbed on the surfaces. As a typical representative of nano-drug and carrier for molecular therapy and diagnosis, the polymer nanoparticles have been widely used for drug delivery system, especially the anti-tumor drugs (13-16).

Poly(ethylene glycol) (PEG) is a non-toxic and non-irritating biopolymer with excellent biocompatibility. It is highly hydrophilic and has good solubility in many organic solvent. The most important is that PEG has a very wide application in biomedical field. It can be used as a solution for contact lens, drug delivery and carrier for immobilized enzyme. The aqueous solution of PEG can be used to cover pill to control the diffusion of drug in vivo and to improve the effect of the drug. PEG is also used for surface modification (i.e. surface absorption and grafting) of medical polymer materials, the modified surface can improve the biocompatibility of the polymer which directly contact with blood (3,5,7-13).

In this paper, PEG end-capped with hexadecane (C16-PEG-C16) was synthesized. This associating polymer is able to form micelle in aqueous solution. The critical micelle concentration of C16-PEG-C16 was determined using pyrene fluorescence. Pyrene was also used as a drug model to prepare pyrene-loaded C16-PEG-C16 polymeric micelle and to investigate the total pyrene concentration in plasma, liver, spleen, lung and kidney of Sprague-Dawley rats. To the best of our knowledge, this is the first study on using pyrene-loaded micelle to determine pyrene concentration in blood and tissues. This research provides a fundamental study for applying fluorescence probe for molecular therapy and diagnosis.

Materials and Methods

Materials

Distilled in glass N,N-dimethylformamide (DMF), tetrahydrofuran (THF), toluene, dichloromethane, diethyl ether and HPLC grade methanol (MeOH) were purchased from Sinopharm Group Co Ltd (Beijing, China). All solvents were used as received. The poly(ethylene oxide) (Mn = 25,000 g/mol) sample, *p*-toluenesulfonyl chloride (98%), triethylamine (98%), sodium hydride (60%, dispersed in oil), hexadecanol (98%) and 1-pyrenemethanol (98%) were purchased from Aldrich.

Animals

SPF grade male Sprague-Dawley (SD) rats (age: 5-6 weeks, weight: 170-200 g) were purchased from Animal Center of Beijing Medical University.

Synthesis of C16-PEG-C16 construct

The synthesis procedure was divided into two steps. First, the hydroxyl ends of the PEG were reacted with *p*-toluenesulfonyl chloride (TsCl) to yield Ts-PEG-Ts. In next step, the toluenesulfonyl moiety of Ts-PEG-Ts were displaced by an excess of sodium hexadecoxide to yield the PEG bearing two hexadecanes. The synthesis procedure is described in detail as follows.

In a round bottom flask, PEG was dissolved into 20 mL of freshly distilled dichloromethane. The solution was kept under N_2 atmosphere. Triethylamine was added to the solution after the dissolution of PEG was complete. The flask was immersed in an ice bath and the mixture was stirred for around 20 min. TsCl was added in small increments. After a few hours, the ice bath was removed and the reaction was allowed to warm to room temperature and left to stir overnight under a nitrogen atmosphere. On the following day, the mixture was concentrated under vacuum and added dropwise to a large amount of diethyl ether. The white precipitate (Ts-PEG-Ts) was filtered and dried in a vacuum oven at room temperature for 12 h. The dry Ts-PEG-Ts was ground into a powder, suspended in 20 mL toluene and stirred for 1-2 h. The impurities, including triethylamine hydrochloride and TsCl residues, were filtered off and the filtrate was rotary evaporated to ca. 5 mL and added dropwise to a large amount of diethyl ether. The white precipitate was collected by filtration and dried for several days.

Ts-PEG-Ts. ^{1}H NMR (300 MHz, DMSO-*d6*), δ (ppm): 7.4 (d, ~4H, ArH), 7.7 (d, ~4H, ArH), 4.1 (t, ~4H, -CH2-), 3.2-3.7 (many small peaks, H from units close to the PEG ends), 3.5 (s, massive peak, H from backbone), 3.3 (m, H_2O).

Hexadecanol was dissolved into 20 mL of freshly distilled DMF in a round-bottom flask. The flask was inflamed beforehand several times under vacuum to completely remove any moisture and it was kept under a nitrogen atmosphere. Sodium hydride was added and the mixture was stirred in the dark at room temperature for 1-2 h. Ts-PEG-Ts was added to the reaction flask which was then placed in an oil bath at 60 ºC and stirred overnight under nitrogen. The oil bath was removed and the mixture was cooled to room temperature after quenching the reaction with a drop of water. The solution was concentrated and precipitated into a large amount

of diethyl ether, the white solid (C16-PEG-C16) was collected from filtration and dried at room temperature under vacuum for 12 h. To remove the sodium tosylate by-product, C16-PEG-C16 was dissolved in 10 mL of dichloromethane and washed three times with 30 mL of water. The organic layer was collected and dried over $MgSO_4$ powder. The solution was concentrated to 5 mL and then precipitated in a large amount of diethyl ether. The precipitate was filtered and dried under vacuum at room temperature for overnight. C16-PEG-C16 was dissolved in methanol at room temperature and the solution was cooled and kept at 0 ºC for overnight, which are the conditions for crystallization of PEG. The white precipitate of C16-PEG-C16 was filtered, re-dissolved in methanol at room temperature and recrystallized by decreasing the temperature to 0 ºC three more times to remove unreacted hexadecanol and its derivatives. After the final precipitation, the solid was dried at room temperature under vacuum for several days. The disappearance of the peaks at 4.5 and 4.1 ppm suggests that PEG chains were successfully modified.

C16-PEG-C16. ^{1}H NMR (300 MHz, DMSO-*d6*), δ (ppm): 0.8-1.2 (~66H, hexadecane H's), 3.2-3.7 (many small peaks, H from units close to the PEG ends), 3.5 (s, massive peak, H from backbone), 3.3 (m, H_2O).

Preparation of pyrene-loaded polymeric micelle

Pyrene-loaded polymeric micelle was prepared by dialysis. First, 20 mg C16-PEG-C16 polymer was dissolved into water, 1-pyrenemethanol (20 mg/mL) in ethanol solution was then added dropwise into the polymer aqueous solution under stirring, the stirring status was kept for overnight. The mixture was then loaded into a dialysis bag with a cutoff molecular weight of 5,000 g/mol and dialyzed against Millipore water for 4-5 days. The water was refreshed 3 times per day. The solution was centrifuged for 8 min at 5,000 r/min. The pyrene-loaded polymeric micelle solution was obtained from the supernatant.

Steady-state pyrene fluorescence

The steady-state fluorescence spectra were acquired using a continuous Xe lamp for excitation that was fitted on a Photon Technology International (PTI) LS-500 steady-state fluorometer.

The pyrene-loaded polymer solution was excited at wavelength of 344 nm with the steady-state emission being monitored from 350 to 600 nm. The slit of the excitation and emission monochromators were set to equal 1.0 nm. The I_3/I_1 ratio was determined from the ratio of the third peak at 386 nm to the first peak at 386 nm.

Encapsulation efficiency and pyrene loading content determination

The pyrene content in polymeric micelle was determined by pyrene steady-state fluorescence. The fluorescence intensity of pyrene is proportional to pyrene concentration. After acquiring the fluorescence spectra of sample solutions, the encapsulation efficiency and pyrene loading content can be determined according to Eqs 1 and 2.

$$\text{Encapsulation efficiency} = \frac{\text{Amounts of pyrene in polymeric micelle}}{\text{Total amounts of pyrene}} \times 100\% \quad (1)$$

$$\text{Pyrene loading content} = \frac{\text{Amounts of pyrene in polymeric micelle}}{\text{Total amounts of pyrene - loaded micelle}} \times 100\% \quad (2)$$

Pretreatment and determination of biological samples

The heart, liver, spleen, lung and kidney samples were taken from SD rats. The samples were precisely weighed and added into physiological saline to prepare 10% homogenate respectively. Homogenates (0.6mL and 0.4mL for liver homogenate) and plasma (120 μL) were precisely taken and 20 μL diazepam internal standard solution with different concentrations were added into the homogenates and plasma. After homogeneously mixing, tert butyl ether (5 mL) was added and centrifuged for 20 min at 2000 r/min. Organic phase (5 mL) was dried at 30 °C under vacuum. The residues were dissolved into 100 μL mobile phase and centrifuged for 20 min at 8,000r/min. The supernatants (25 μL) were taken and analyzed as experimental samples.

Standard Curve

The homogenate samples of plasma, heart, liver, spleen, lung and kidney were carefully taken and added into different amounts of stock solutions to prepare the standard solutions with different concentrations. Other procedures followed the steps described in the section of "Pretreatment and determination of biological samples". The intensity of fluorescence peak of samples and internal standard peak were recorded, linear regression of drug concentration in plasma or tissue homogenates was conducted according to the ratio of peak intensity or peak area, the regression equation of plasma and tissues samples were obtained.

Results

Characterization of C16-PEG-C16 polymeric micelle

The C16-PEG-C16 polymer synthesized in this study is a typical amphiphilic polymer. The PEG backbone is hydrophilic while the hexadecane chain ends are hydrophobic. at very low concentration, the polymer chains are present in solution as dissociated unimers. When the concentration is increased to the critical micelle concentration (CMC), the hydrophobes associate resulting in the formation of micelles. The CMC is a very important parameter for polymer micelle and it can be determined by pyrene fluorescence.
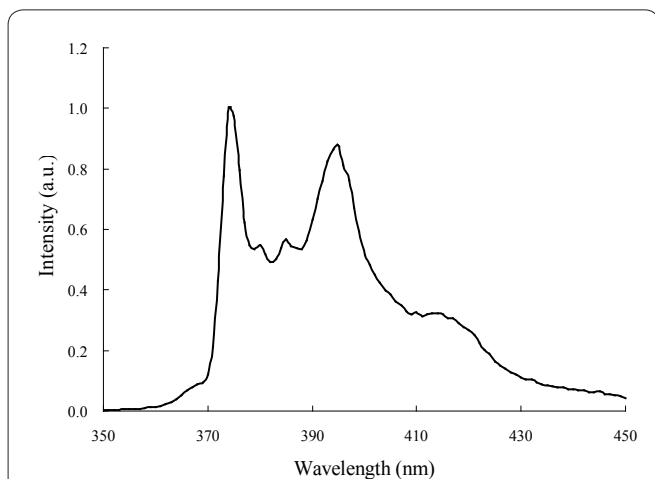

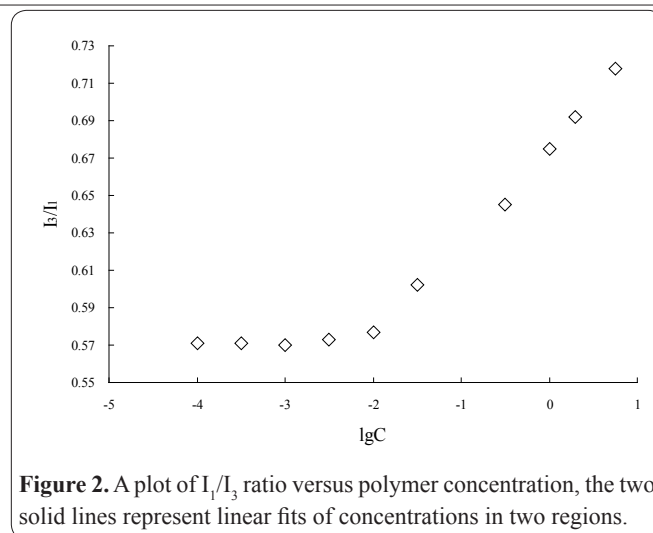**Figure 1.** Fluorescence emission spectrum of pyrene monomer.

Figure 2. A plot of I_1/I_3 ratio versus polymer concentration, the two solid lines represent linear fits of concentrations in two regions.

Upon excitation, an excited pyrene monomer can deactivate itself by returning to the ground-state via fluorescence. Figure 1 shows a typical emission spectrum of pyrene monomer.

As show in Figure 1, the emission spectrum of excited pyrene monomer exhibits four peaks. The ratio of the first peak (at 374 nm) and the third peak (at 385 nm) is strongly dependent with the polarity of the microenvironment in where pyrene is located, the I_1/I_3 ratio is usually used to investigated formation of polymeric micelle. In this paper, 1-pyrenemethanol was added into C16-PEG-C16 polymer aqueous solution with different polymer concentrations. After acquiring steady-state fluorescence emission spectra at all concentrations, the I_1/I_3 ratios were calculated and plotted with polymer concentration.

Figure 2 shows a plot of I_3/I_1 ratio obtained at various C16-PEG-C16 concentration versus polymer concentration. Two regions can be clearly observed in Figure 2, at low polymer concentrations the ratio is small and independent with polymer concentration, while at higher concentrations, the ratio increases with polymer concentration, suggesting that the polarity of the microenvironment solubilizing pyrene was different in the two regions. By linearly fit the data of I_3/I_1 with log value of polymer concentration, the onset polymer concentration was determined to equal 0.0063 mg/mL, indicating that CMC of C16-PEG-C16 polymer is 0.0063 mg/mL.

Figure 3 shows transmission electron microscopy (TEM) image of C16-PEG-C16 at a concentration of 0.01 mg/mL, the concentration is greater than the CMC of the polymer. Spherical and uniform micelles can be observed in Figure 3, the diameters of the formed nanoparticles are less than 100 nm.
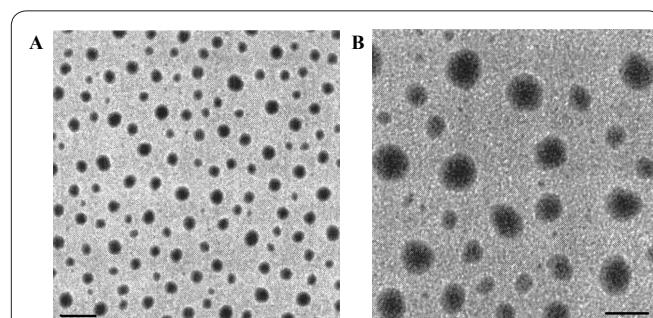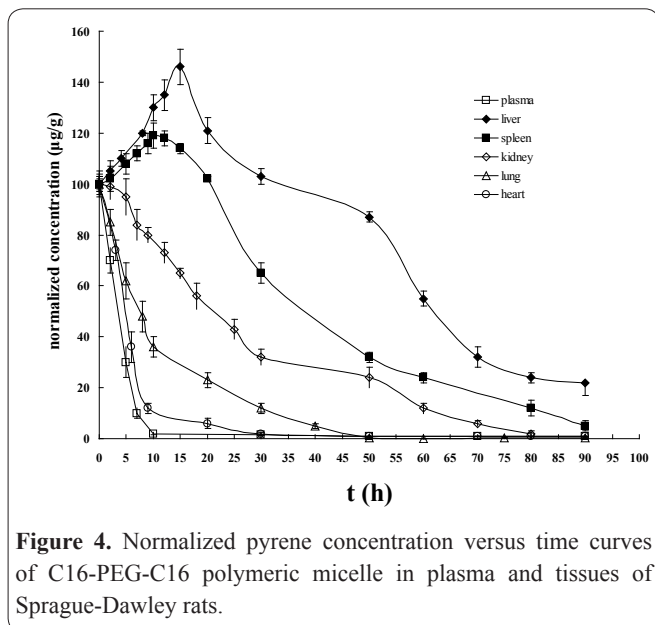

Figure 3. TEM image of C16-PEG-C16 polymeric micelle. (A) Scale bar = 0.5 μm, (B) Scale bar = 0.1 μm.

Table 1. The regression equations of various biological samples.

sample	linear range	regression equation	correlation coefficient (r =)
plasma	0.06 - 116	$0.0457C - 0.0132$	0.9998
liver	0.05 - 86	$0.3285C - 0.0089$	0.9994
lung	0.05 - 22	$0.0612C - 0.0007$	0.9998
kidney	0.05 - 49	$0.0337C - 0.0044$	0.9995
heart	0.05 - 3	$0.4275C - 0.0023$	0.9996
spleen	0.05 - 16	$0.2079C - 0.0144$	0.9995

Figure 4. Normalized pyrene concentration versus time curves of C16-PEG-C16 polymeric micelle in plasma and tissues of Sprague-Dawley rats.

Regression equations of different biological samples

According to the procedures described in experimental section, the linear ranges, regression equations and correlation coefficient of plasma and various tissues were obtained and listed in Table 1.

Drug decay curves

The contents of pyrene were determined according to steady-state fluorescence intensity of various samples. Pyrene concentrations in the biological samples including plasma, liver, spleen, lung and kidney of Sprague-Dawley rats were plotted versus time to estimate the distribution of pyrene in vivo. The curves were shown in Figure 4, the initial concentrations were normalized for comparison.

Discussion

In this paper, the dialysis method was selected to investigate the drug loading process of the C16-PEG-C16 polymeric micelle, the results showed that the polymer micelles have a superior drug loading capacity. The encapsulation efficiency reached 83.4% and the drug loading content reached 36.1%, which represents a high level for the research of paclitaxel polymeric micelles. The drug concentration in plasma of SD rats rapidly reduced after intravenous injection of C16-PEG-C16 polymeric micelle, the micelles did not show a long-loop property of general polymer micelles, the possible reason is that the structure of polymeric micelle in this study is different with the general block copolymers, which form polymeric micelle with a long hydrophilic chain stretching to external space of micelle, consequently the carrier contains a hydrophilic surface but the steric hinderance and surface flexibility simulta-

neously increase. The adhesion of colloidal particles to regulatory protein in blood weakens to reduce the recognition of mononuclear cells, and the polymer structure is connected with hydrophobic chains. A large number of hydrophilic groups and non-hydrophilic flexible long chains are formed after the formation of micelles, which leads to the rapid decrease of serum and plasma concentrations.

C16-PEG-C16 exhibited a high affinity to liver and spleen, drug concentration in blood decreased rapidly after drug administration. After 15 min, it already reduced to 0.74% of initial dose. At the same time, the drug concentration in liver increased rapidly and reached a maximum in 15 min, the distribution was 85.8% of drug concentration of administration. This relationship of drug concentration between blood and liver was in agreement with the study of the liver-targeted nanoparticles. After C16-PEG-C16 administration, the drug concentration in blood decreased rapidly. During the period of 15-30 min, an increase in drug distribution was not mainly due to an uncharged C16-PEG-C16 surface, the vascular wall contains a large number of negatively charged glycosam inoglycans, they can not interact with each other. Therefore, the micelle can adhere to the vascular wall and continues to release drugs using vascular wall as a drug reservoir.

C16-PEG-C16 polymeric micelles have a high affinity to liver and a strong liver retention characteristics. The liver intake reached maximum (89.2% of the dose) after 15 min of drug administration, and then slowly decreased, after 48 h and 128 h, the liver volume is still accounted for 24.5%. After 30 min, the liver uptake was 58.7% of the dose. After 72 h drug concentration was lower than the detection limit, suggesting that C16-PEG-C16 has strong liver targeting and retention characteristics in liver. C16-PEG-C16 reached a maximum distribution (4.82% of the dose) in the spleen after 15 min of drug administration, suggesting that C16-PEG-C16 has also good targeting and retention characteristics in spleen.

The main toxicity of some drugs include the inhibition of bone marrow, heart and kidney toxicity. In this paper, it was found that the distribution of C16-PEG-C16 polymeric micelle in heart and kidney is not significant. The highest drug distribution in the heart and kidney of polymer was only 0.57% and 0.46%, respectively. The decrease in cardiac and renal toxicity has important implications for the clinical application of the polymeric micelle.

C16-PEG-C16 polymeric micelles is a new drug carrier in the field of pharmaceutical and biological research. In this study, the C16-PEG-C16 polymer was successfully prepared and the influence factors on the distribution of the polymeric micelles in SD rats were investigated. C16-PEG-C16 showed high affinity and

retention characteristics of liver and spleen. The polymer has a better targeting in lung, the distribution of the heart and kidney are very low, consequently the toxic side effects of drugs on these organs are significally reduced. This study is extremely important to the clinical treatment o liver, spleen and lung diseases.

References

1. Alexis F, Rhee JW, Richie JP, Radovic-Moreno AF, Langer R, Farokhzad OC. New frontiers in nanotechnology for cancer treatment. Urol Oncol - Semin Ori 2008; 26: 74-85.

2. Park JH, Lee S, Kim JH, Park K, Kim K, Kwon IC. Polymeric nanomedicine for cancer therapy. Prog Polym Sci 2008; 33: 113-37.

3. Parveen S, Sahoo SK. Polmeric nanoparticles for cancer therapy. J Drug Target 2008; 16: 108-23.

4. Pridgen EM, Langer R, FarokhZad OC. Biodegradable, Polymeric nanoparticle delivery systems for cancer therapy. Nanomedicine 2007; 2: 669-80.

5. Christine V, Kawthar B. Methods for the preparation and manufacture of polymeric nanoparticles. Pharm Res 2009; 26: 1025-58.

6. Pinto RC, Neufeld RJ, Ribeiro AJ, Veiga F. Nanoencapsulation I. Methods for preparation of drug-loaded polymeric nanoparticles. Nanomedicine 2006; 2: 8-21.

7. Anton N, Benoit JP, Saulnier P. Design and production of nanoparticles formulated from nano-emulsion templates - A review. J Control Release 2008; 128: 185-99.

8. Anton N, Gayet P, Benoit JP, Saulnier P. Nano-emulsions and nanocapsules by the PIT method: an investigation on the role of the temperature cycling on the emulsion phase inversion. Int J Pharm 2007; 344: 44-52.

9. Bouchemal K, Briancon S, Fessi H. Nanoemulsion formulation using spontaneous emulsification: Solvent, oil and surfatant optimization. Int J Pharm 2004 ; 280: 241-51.

10. Desgouilles S, Vauthier C, Bazile D, Vacus J, Grossiord J, Veillard M et al. The design of nanoparticles obtained by solvent evaporation: a comprehensive study. Langmuir 2003; 19: 9504-10.

11. Leroux JC, Allemann E, Doelker E, Gurny R. New approach for the preparation of nanoparticles by an emulsification-diffusion method. Eur J Pharm BioPharm 1995; 41: 14-8.

12. Allemann E, Gurnay R, Doelker E. Preparation of agueous polymeric nanodispersions by a reversible salting-out proeess: influence of process parameters on particle size. Int J Pharm 1992; 87: 247-53.

13. Allemann E, Leroux JC, Gurnay R, Doelker E. In vitro extended-release properties of drug-loaded poly(D, L-lactic acid) nanoparticles produced by a salting-out procedure. Pharm Res 1993; 10: 1732-7.

14. Legrand P, Lesieur S, Bochot A, Gref R, Raatjes W, Barratt G et al. Influence of polymer behaviour in organic solution on the production of polylactide nanoparticles by nanoprecipitation. Int J Pharm 2007; 344: 33-43.

15. Michael CM, Ilia F, Danenberg HD, Gershon G. Study of the drug release mechanism from tyrphostin AG-295-loaded nanospheres by in situ and external sink methods. J Control Release 2002; 83: 401-14.

16. Galindo-Rodriguez SA, Eric A, Fessi H, Eric D. Polymeric nanoparticles for oral deliver of drugs and vaccines: a critical evaluatio of in vivo studies. Crit Rev Ther Drug 2005; 2: 419-64.

17. Zamboni WC. Liposomal, nanoparticle, and conjugated formulations of anticancer agents. Clin Cancer Res 2005; 11: 8230-4.